# Tracking and Stabilization of Heart-rate using Pacemaker with FOF-PID Controller in Secured Medical Cyber-physical System

Pritam Khan, Yasin Khan, Sudhir Kumar
Department of Electrical Engineering
Indian Institute of Technology Patna, India
Email:{pritam_1921ee05, khyasin, sudhir}@iitp.ac.in

***Abstract*—In this paper, we design and analyze a control system to mitigate the fluctuations and regulate the heart rate using pacemaker. We use Fractional Order Fuzzy-Proportional-Integral-Derivative (FOF-PID) controller which generates electric pulses to maintain the desired heart rate by minimizing unprecedented fluctuations of the beats. The proposed control model is compared with the pacemakers using Fractional Order-PID (FO-PID) and Fuzzy-PID (F-PID) controllers. FOF-PID controller proves its superiority in performance over the existing controllers. Real-time tracking of heart-rate through IoT network enables easy communication between patient and healthcare unit possibly preventing a mishap. The maximum percentage of error is 0.72 for FOF-PID controller while the same is 3.14, 6.18 and 23.26 using FO-PID, F-PID and PID controllers respectively in a male heart. For a female heart, the maximum error percentages are 1.55, 2.13, 11.25 and 24.38 using FOF-PID, FO-PID, F-PID and PID controllers respectively. Finally, data anonymity is used to secure the data in the medical cyber-physical system.**

***Index Terms*—Cyber-physical system, controller, fractional calculus, fuzzy, pacemaker.**

## I. Introduction

Arrhythmia and cardiac failures are a leading cause of death worldwide. Artificial cardiac pacemaker (ACP) and implantable cardioverter defibrillator (IDC) are devices which when implanted within a cardiac patient, help in pacing the heart at the normal rhythm. Those devices help in preventing fibrillation by monitoring the heart-rate at real time and communicate with medical experts/devices as a part of cyber-physical systems [1]. Cyber-physical systems find rapid adoption in medical applications (viz. heart-rate monitoring, e-medicine, e-consults, and biomedical database) thereby creating a smart healthcare system [2]. In this work, an FOF-PID controller is tuned to mitigate the fluctuations of heart-rate. The traditional PID controller does not provide the craved outcomes for complex and non-linear systems [3]. However, FO-PID and F-PID controllers overcome the disadvantages of traditional PID Controller and achieve a better performance. The proposed method using a combination of fractional, fuzzy and PID controllers proves to be the best. System non-linearities and unpredictability issues are overcome using the FOF-PID controller. Zeigler-Nichols (Z-N) and Tyreus-Luyben (T-L) tuned FO-PID and F-PID controllers are presented in [4] but the overshoot issue is still not eliminated. Although a mathematical approach is taken for pacemaker control in

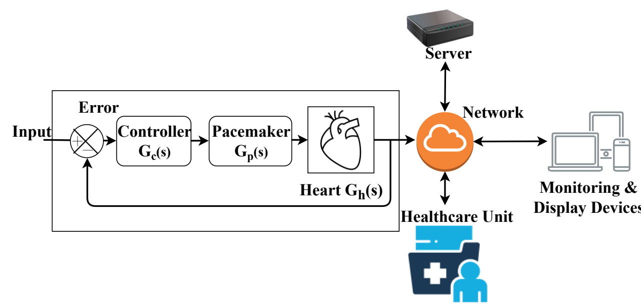


Fig. 1: Artificial cardiac pacemaker in cyber-physical system

[5], the usage of the R-R interval of electrocardiogram (ECG) waveform limits the robustness of the control system. In cyber-physical domain, the application of health monitoring is discussed in few works [6]. However, stabilization of heart-rate is rarely implemented in the cyber-physical sector. Although the usage of FOF-PID controller in heart-rate stabilizing is novel in our work, the FOF-PID controller is used for load frequency regulation in [7].

### A. Contributions

The contributions of this work are enumerated as follows:

1) We propose an implantable pacemaker with an FOF-PID controller that eliminates the overshoot in the heart-rates. The FOF-PID controller is more accurate compared to PID, FO-PID or F-PID controller for pacing and correcting heart-rate of a cardiac patient.
2) The fractional order differential equation, fuzzy logic and PID controller are used in FOF-PID controller. The expressions for fractional orders are obtained by minimizing overshoot.
3) The numerical results of the proposed FOF-PID controller outperform the state-of-the-art controllers.

The rest of the paper is presented as follows: Section II describes the mathematical model of heart. Section III presents the designing of FOF-PID controller for cardiac pacemaker. Simulation and experimental results are discussed in Section IV. Finally, a brief conclusion and future work are highlighted in Section V.

978-1-7281-3187-0/20/$31.00 ©2020 IEEE

Authorized licensed use limited to: SUNY AT STONY BROOK. Downloaded on September 22,2021 at 04:08:15 UTC from IEEE Xplore. Restrictions apply.

## II. Stabilizing of Heart-rate using FOF-PID Controller in a Secured Healthcare Unit

### A. Heart Modeling using Pacemaker

The transfer functions of controller, pacemaker and heart together contribute to the heart-rate stabilization system. The pacemaker is a first-order linear time variant system which can be represented as:

$$G_p(s) = \frac{k}{1+s\tau} \tag{1}$$

where $k$ and $\tau$ represent the steady-state gain and time-constant respectively. The transfer function of the pacemaker is considered to be a low pass filter with $\tau = 1/8$ second and $k = 1/8$ [3]. It is given by: $G_p(s) = \frac{8}{s+8}$. The functioning of the heart can be represented by the differential equation in Laplace domain:

$$Ms^2X(s) + BsX(s) + KX(s) = F(s) \tag{2}$$

where $M$ is the mass of cardiac muscle, $B$ and $K$ are the constants of proportionality for viscous drag and torsional drag of myocardial cell respectively. $F(s)$ is the force exerted by the cardiac muscle specimen and this force is generated by the electrical and electrochemical activity causing a displacement of $X(s)$ on the cardiovascular system. Equation 2 can be written as:

$$G_h^c(s) = \frac{X(s)}{F(s)} = \frac{1}{Ms^2+Bs+K} \tag{3}$$

where $G_h^c(s)$ represents the closed loop transfer function of heart considering unity feedback. Equation 3 can be compared with a standard second order control system:

$$\frac{X(s)}{F(s)} = \frac{\omega_n^2}{s^2+2\zeta\omega_n s+\omega_n^2} \tag{4}$$

where $\zeta$ is the damping coefficient and $\omega_n$ is the undamped natural frequency of oscillation of a second order closed loop control system. Comparing the characteristic equations from Equations 3 and 4, we get $\omega_n = \sqrt{1/M} = \sqrt{K/M}$, $\zeta = \frac{B}{2\sqrt{M}}$. The damped frequency of oscillation $\omega_d = \omega_n\sqrt{1-\zeta^2}$. Considering the heart-rate as 72 beats per minute, that is, $f_d = \frac{72}{60} = 1.2$ Hz, we have the damped frequency of oscillation of heart as $\omega_d = 2\pi f_d = 7.54$ radian/second. Considering the value of the damping coefficient $\zeta = 0.8$, we get:

$$\omega_n = \frac{\omega_d}{\sqrt{1-\zeta^2}} = \frac{7.54}{\sqrt{1-.64}} = 12.57 \text{ rad/sec} \tag{5}$$

Now, putting the values of $\zeta$ and $\omega_n$ in the forward path transfer function of a unity feedback second order system, we get:

$$\frac{\omega_n^2}{s(s+2\zeta\omega_n)} = \frac{12.57^2}{s(s+2(.8)12.57)} = \frac{158}{s^2+20.11s} \tag{6}$$

which is close to the actual transfer function of heart $G_h(s) = \frac{169}{s(s+20.8)}$ [3]. Therefore, practically the transfer function varies depending on the damping coefficient and damped frequency of oscillation.

### B. Closed Form Expressions for Fractional Orders

The general expression of an FO-PID controller shown in Figure 2(a) is given by:

$$u(t) = K_pe(t) + K_dD^{\mu}e(t) + K_iD^{-\lambda}e(t) \tag{7}$$

where $K_p$, $K_d$ and $K_i$ are proportional, derivative and integral gains respectively, $u(t)$ is the controller output, $e(t)$ is the input error signal in time-domain. The block diagram of the heart-rate stabilizing system using FOF-PID controller is shown in Figure 2(b). The FOF-PID controller transfer function is represented as $G_c(s)$ in Figure 1. In order to get

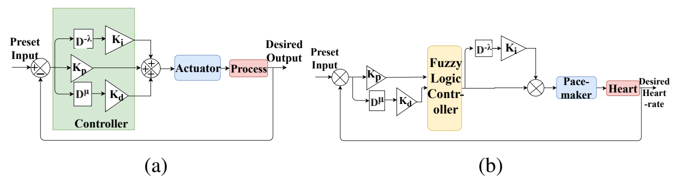


Fig. 2: Block diagram of (a) FO-PID control system (b) proposed FOF-PID control system

the optimal value of $\mu$ and $\lambda$ for which we have the minimum value of overshoot, we integrate the squared overshoots over time $T$. $K$ is the steady heart-rate value. Therefore, overshoot $M(t)$ is given by: $M(t) = K - u(t_p)$. For the sake of simplicity, we consider $t_p$ as $t$ in further expressions. Now, integrating the square of overshoots over time $T$, we get:

$$\frac{1}{T}\int_0^T M^2(t)dt = \frac{1}{T}\int_0^T (K-u(t))^2dt \tag{8}$$

We differentiate Equation 8 partially with respect to $\mu$ and $\lambda$ to obtain their optimum values. Hence, on differentiating with respect to $\mu$ we get:

$$\frac{\partial}{\partial\mu}\left[\frac{1}{T}\int_0^T (K-u(t_p))^2dt\right] = 0 \tag{9}$$

Similarly, we differentiate Equation 8 with respect to $\lambda$. The fractional values of $\mu$ and $\lambda$ are kept between 0 and 1. However, as the controller approaches steady-state, the effect of derivative control dies out and that due to proportional and integral prevails. The time-complexity of the controller is of the order of $O(n)$ where $n$ is the number of floating-point operations for the root mean squared error to get calculated by the controller before achieving steady-state. Same is the order of time-complexity for FO-PID, F-PID and PID controllers for arriving at steady-state value.

### C. Fuzzy Logic Controller

In the FOF-PID controller, for FLC block, the system error $e(t)$ and the fractional order derivative of error $D^{\mu}e(t)$ are given as inputs. The output of FLC, which is pace here, is then fed to the fractional order integral part. There are seven crisp inputs and seven crisp outputs. The triangular membership functions for both input and output in Mamdani type inference system are considered for the controller. Figure 4(a) gives the input membership functions while Figure 4(b) represents the output membership function and Table I gives 49 rules for the fuzzy controller.

Authorized licensed use limited to: SUNY AT STONY BROOK. Downloaded on September 22,2021 at 04:08:15 UTC from IEEE Xplore. Restrictions apply.

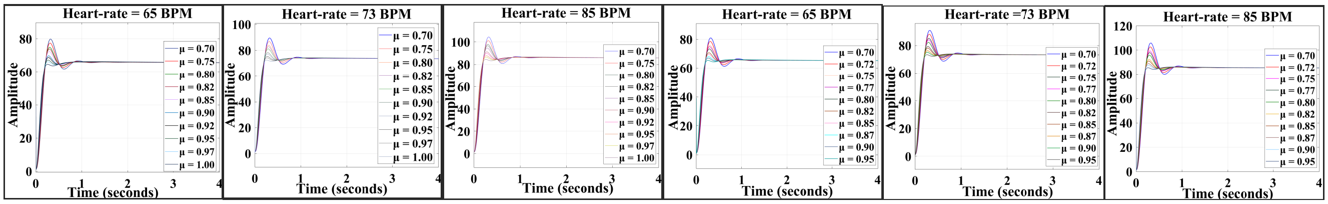


(a) (b) (c) (d) (e) (f)

Fig. 3: (a), (b), (c): Different overshoots for different $\mu$ for $\lambda = 0.75$ at different heart-rates in resting condition, (d), (e), (f): Different overshoots for different $\mu$ for $\lambda = 0.65$ at different heart-rates in resting condition

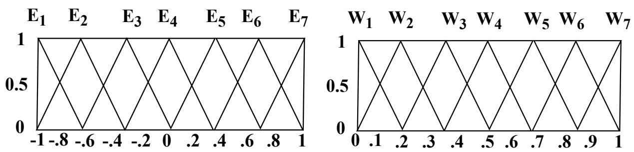


(a) (b)

Fig. 4: (a) Membership function value $\Psi(x)$ vs. input value $x$, where $x$ is either error or change of error (b) Membership function value $\Psi(x)$ vs. FLC output value

TABLE I: Fuzzy rule base

| $\mathbf{e(t)}$ \ $\Delta\mathbf{e(t)}$ | $\mathbf{E_1}$ | $\mathbf{E_2}$ | $\mathbf{E_3}$ | $\mathbf{E_4}$ | $\mathbf{E_5}$ | $\mathbf{E_6}$ | $\mathbf{E_7}$ |
|---|---|---|---|---|---|---|---|
| $\mathbf{E_1}$ | $W_7$ | $W_7$ | $W_7$ | $W_3$ | $W_2$ | $W_2$ | $W_1$ |
| $\mathbf{E_2}$ | $W_7$ | $W_7$ | $W_6$ | $W_4$ | $W_3$ | $W_3$ | $W_3$ |
| $\mathbf{E_3}$ | $W_7$ | $W_5$ | $W_5$ | $W_6$ | $W_2$ | $W_6$ | $W_6$ |
| $\mathbf{E_4}$ | $W_6$ | $W_5$ | $W_7$ | $W_1$ | $W_7$ | $W_5$ | $W_5$ |
| $\mathbf{E_5}$ | $W_4$ | $W_4$ | $W_3$ | $W_6$ | $W_5$ | $W_5$ | $W_7$ |
| $\mathbf{E_6}$ | $W_3$ | $W_3$ | $W_3$ | $W_4$ | $W_6$ | $W_7$ | $W_7$ |
| $\mathbf{E_7}$ | $W_1$ | $W_2$ | $W_2$ | $W_3$ | $W_7$ | $W_7$ | $W_7$ |

The rule base for the proposed controller is given in Table I. An example of the fuzzy rules from Table I is as follows: if $e(t)$ = $E_1$ and $\Delta e(t)$ = $E_2$, then the pace or decision is $W_7$. In defuzzification process, the FLC transforms the fuzzy output into crisp output. We use the weighted average method [8] in the proposed work for defuzzification which is defined as follows:

$$Z = \frac{\sum_i x_i \cdot \Psi(x_i)}{\sum_i \Psi(x_i)} \tag{10}$$

where $Z$ = controller crisp output value, $x_i$ = controller fuzzy input value and $\Psi(x)$ = degree of the membership value.

### *D. Data Security in Healthcare Unit*

The sensing and controlling action needs to be monitored by the healthcare units for the treatment of the cardiac patient. There remains the possibility of data theft from the healthcare unit thereby posing a threat to the privacy and security issues. We use $k$-anonymization technique where $k$ denotes the minimum number of records that look similar after anonymization [9]. In $k$-anonymization technique, two methods are used namely, suppression and generalization. Each row is a record or tuple while each column denotes an attribute. After anonymization, each tuple must be identical to at least $k-1$ tuples of the anonymized dataset. The attributes can be sensitive, quasi-sensitive or insensitive. The sensitive attributes must not be available to the adversary whereas the insensitive attributes and quasi-sensitive attributes can be kept open.

TABLE II: Root-mean squared error (RMSE) and maximum error for different controllers with respect to reference heart-rate

| | Female-heart | | Male-heart | |
|---|---|---|---|---|
| **Controller** | **RMSE** | **Maximum Error %** | **RMSE** | **Maximum Error %** |
| **FOF-PID** | 0.55 | 1.55 | 0.49 | 0.72 |
| **FO-PID** | 0.72 | 2.13 | 1.58 | 3.14 |
| **F-PID** | 2.53 | 11.25 | 3.62 | 6.18 |
| **PID** | 4.32 | 24.38 | 4.165 | 23.26 |

## III. Numerical Results and Discussion

The Simulink model is considered using different controllers for static and varying heart-rates. The values of $\mu$ and $\lambda$ are considered from 0.7 to 1 by intervals of 0.02 and 0.05. Figure 3(a), 3(b), 3(c) and 3(d), 3(e), 3(f) show the plots by varying $\mu$ and $\lambda$. Minimum overshoot/undershoot is attained for $\frac{\mu}{\lambda} \approx 1.2$ in all cases.

Figure 5 shows the improvement in overshoot minimization for different controllers with optimized $\mu$ and $\lambda$ at different heart-rates using fuzzy membership function as shown in Figure 4. Maximum error % and root mean squared error (RMSE) for varying heart-rates of male and female using different controllers are calculated from Figure 6 and shown in Table II. The energy consumption in simulating the controllers is about $1.56 \times 10^{-3} \mu$W per FLOP (floating point operation) in a computer with Intel i5-4200U processor operating at 2.30GHz.

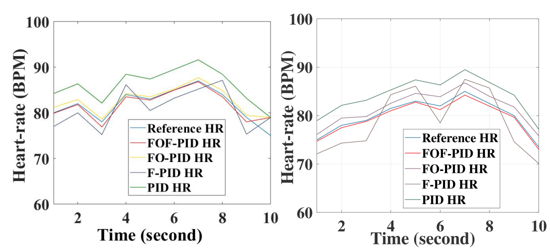


(a) (b)

Fig. 6: Varying heart-rates using different controllers for (a) female (b) male

Authorized licensed use limited to: SUNY AT STONY BROOK. Downloaded on September 22,2021 at 04:08:15 UTC from IEEE Xplore. Restrictions apply.

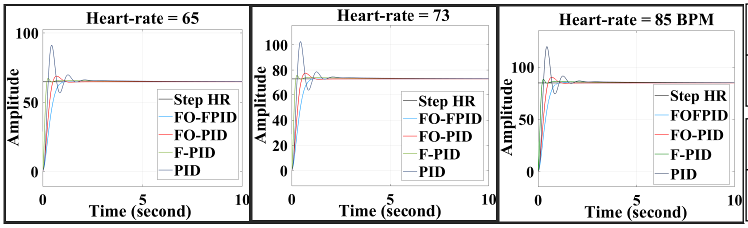


(a) (b) (c)

| Original Data | Male | 75 | 700135 | 58 |
|---|---|---|---|---|
| Representation ($D_1$) | 1 | 1 | 1 | 1 |

| Anonymized Data | Person | $\geq 70$ | 700100-700399 | * |
|---|---|---|---|---|
| Representation ($D_1^*$) | 1 | 1 | 1 | 0 |

(d)

Fig. 5: (a), (b), (c) Performance comparison of different controllers at different heart-rates with optimized $\mu$ and $\lambda$ (d) Similarity of 1st record of Table III and Table IV

TABLE III: Cardiac patient data with attributes

| Pacemaker ID | Gender | Age | Heart-rate | Temperature | Status |
|---|---|---|---|---|---|
| 40012 | Female | 52 | 72 | 98 | Normal |
| 40013 | Male | 55 | 69 | 99 | Normal |
| 40018 | Female | 58 | 71 | 97 | Normal |
| 40020 | Male | 59 | 73 | 100 | Normal |
| 40021 | Male | 56 | 48 | 97 | Abnormal |
| 40023 | Male | 69 | 83 | 97 | Normal |
| 40027 | Female | 61 | 53 | 97 | Abnormal |

TABLE IV: Cardiac patient data with 2-anonymity

| Pacemaker ID | Gender | Age | Heart-rate | Temperature | Status |
|---|---|---|---|---|---|
| 4001* | Person | [50, 60] | * | * | Normal |
| 4001* | Person | [50, 60] | * | * | Normal |
| 4001* | Person | [50, 60] | * | * | Normal |
| 4002* | Person | [50, 60] | * | * | Normal |
| 4002* | Person | [50, 60] | * | * | Abnormal |
| 4002* | Person | [60, 70] | * | * | Normal |
| 4002* | Person | [60, 70] | * | * | Abnormal |

### A. Anonymization of Health Data

Tables III and IV show an example of original and corresponding $k$-anonymized patient dataset respectively with $k = 2$. Different features like “Pacemaker ID”, “Age”, “Gender”, “Heart-rate” and “Temperature” are quasi-sensitive attributes while “Status” is sensitive attribute. Pacemaker ID, heart-rate and temperature are the 3 attributes that are suppressed by ‘*’ while gender and age are generalized. Minimum of 2 records appear identical after using 2-anonymity. However, the sensitive attribute is exempted from anonymization.

We calculate the similarity between $D_1$ and $D_1^*$ in Figure 5(d). We consider every attribute as 1 in representation row of original data. The suppressed attributes denoted by * in anonymized data are considered as 0 considering the worst case that we get erroneous value on de-anonymizing. The generalized attribute values are represented as 1 because the original attribute value is a sub-set of the generalized attribute. For example, 52 is a subset of [50, 60]. Calculating the cosine similarity, we get $\cos(D_1, D_1^*) = \frac{D_1.D_1^*}{|D_1||D_1^*|} = \frac{1.0+1.1+1.1+1.0+1.0}{\sqrt{5}\sqrt{2}} = \sqrt{\frac{2}{5}}$. Assuming similar result for all the 7 records of our dataset, we get a minimum similarity measure of $\text{Sim}(D, D^*) = \sum_{i=1}^{7} \cos(D_i, D_i^*) = 7\sqrt{\frac{2}{5}} \approx 4.43$ where a maximum similarity of 7 can be achieved.

## IV. Conclusion and Future Work

In this work, an FOF-PID controller is optimized for using in conjunction with a pacemaker in the heart of a human being. This controller helps in mitigating the overshoots in heart-rate thereby stabilizing it. Comparison of PID, F-PID, FO-PID and FOF-PID controllers with a preset heart-rate show the superiority of FOF-PID controller over the rest. The RMSE is minimized to 0.55 and 0.49 for female and male hearts respectively using the optimized FOF-PID controller. Optimization of the fractional order derivative and integral of the controller is carried out yielding $\mu \approx 1.2\lambda$ thereby minimizing the overshoot value. Additionally, a secured communication of the cardiac data to the dedicated healthcare units is also ensured using anonymization technique. A prototype using hardware is being developed.

## Acknowledgement

This work acknowledges the support rendered by the Early Career Research (ECR) award scheme project “Cyber-Physical Systems for M-Health” (ECR/2016/001532) (duration 2017-2020), under Science and Engineering Research Board (SERB), Govt. of India.

## References

[1] Z. Liu, Z. Wang, Y. Ren, Q. Feng, D. Fan, and Z. Zuo, “A City Medical Resources Distribution Optimization Platform Based on Cyber Physical Systems (CPS),” in *2018 International Conference on Sensing, Diagnostics, Prognostics, and Control (SDPC)*. IEEE, 2018, pp. 269–273.

[2] S. Meraghni, L. S. Terrissa, S. Ayad, N. Zerhouni, and C. Varnier, “Post-prognostics decision in cyber-physical systems,” in *2018 International Conference on Advanced Systems and Electric Technologies (IC_ASET)*. IEEE, 2018, pp. 201–205.

[3] K. A. Govind and R. A. Sekhar, “Design of a Novel PID Controller for Cardiac Pacemaker,” in *2014 International Conference on Advances in Green Energy (ICAGE)*. IEEE, 2014, pp. 82–87.

[4] S. P. Arunachalam, S. Kapa, S. K. Mulpuru, P. A. Friedman, and E. G. Tolkacheva, “Intelligent fractional-order PID (FOPID) heart rate controller for cardiac pacemaker,” in *2016 IEEE Healthcare Innovation Point-Of-Care Technologies Conference (HI-POCT)*. IEEE, 2016, pp. 105–108.

[5] P. Bogdan, S. Jain, K. Goyal, and R. Marculescu, “Implantable pacemakers control and optimization via fractional calculus approaches: A cyber-physical systems perspective,” in *2012 IEEE/ACM Third International Conference on Cyber-Physical Systems*. IEEE, 2012, pp. 23–32.

[6] L. Shangguan and S. Gopalswamy, “Health monitoring for cyber physical systems,” *IEEE Systems Journal*, 2019.

[7] M. A. G. Mohamed, A. G. M. A. Ghany, A. Bensenouci, M.-A. Bensenouci, and M. N. Syed-Ahmad, “Fuzzy Fractional-Order PID Tuned via Relative Rate Observer for the Egyptian Load Frequency Regulation,” in *2018 Twentieth International Middle East Power Systems Conference (MEPCON)*. IEEE, 2018, pp. 103–109.

[8] T. J. Ross, “Properties of membership functions, fuzzification, and defuzzification,” *Fuzzy logic with engineering applications*, pp. 89–116, 2010.

[9] F. Prasser and F. Kohlmayer, “Putting statistical disclosure control into practice: The arx data anonymization tool,” in *Medical Data Privacy Handbook*. Springer, 2015, pp. 111–148.



Authorized licensed use limited to: SUNY AT STONY BROOK. Downloaded on September 22,2021 at 04:08:15 UTC from IEEE Xplore. Restrictions apply.